

## Effect of Polymer Hygroscopicity on the Phase Behavior of Amorphous Solid Dispersions in the Presence of Moisture

Alfred C. F. Rumondor<sup>†,‡</sup> and Lynne S. Taylor<sup>\*,†</sup>

*Department of Industrial and Physical Pharmacy, School of Pharmacy, Purdue University, West Lafayette, Indiana 47907, and Pharmaceutical Development, AstraZeneca Pharmaceuticals LP, Wilmington, Delaware, 19850*

Received September 10, 2009; Revised Manuscript Received November 11, 2009; Accepted December 29, 2009

**Abstract:** It has been previously observed that exposure to high relative humidity (RH) can induce amorphous–amorphous phase separation in solid dispersions composed of certain hydrophobic drugs and poly(vinylpyrrolidone) (PVP). The objective of this study was to investigate if this phenomenon occurred in solid dispersions prepared using less hygroscopic polymers. Drug–polymer miscibility was investigated before and after exposure to high RH using infrared (IR) spectroscopy and differential scanning calorimetry (DSC). PVP, poly(vinylpyrrolidone-co-vinyl acetate) (PVPVA), and hypromellose acetate succinate (HPMCAS) were selected as model polymers, and felodipine, pimozide, indomethacin, and quinidine were selected as model drugs. Drug–polymer mixing at the molecular level was confirmed for all model systems investigated. Moisture-induced drug–polymer demixing was observed in felodipine–PVPVA, quinidine–PVP, quinidine–PVPVA, pimozide–PVPVA, and pimozide–HPMCAS systems, but was absent in the other HPMCAS dispersions and for indomethacin–PVPVA. It is concluded that the balance between the thermodynamic factors (enthalpy and entropy of mixing) in a ternary water–drug–polymer system is the important factor in determining which solid dispersion systems are susceptible to moisture-induced amorphous–amorphous phase separation. Systems with strong drug–polymer interactions and a less hygroscopic polymer will be less susceptible to moisture-induced phase separation, while more hydrophobic drugs will be more susceptible to this phenomenon even at low levels of sorbed moisture.

**Keywords:** Amorphous solid dispersion; miscibility; moisture; infrared spectroscopy; differential scanning calorimetry

### Introduction

Many new therapeutic compounds have unfavorable physical properties;<sup>1</sup> for example, it has been estimated that as many as 40% of drug molecules have a suboptimum aqueous solubility.<sup>2</sup> This will potentially reduce the dissolution rate of the drug in the gastrointestinal tract, which is

the first step for absorption of the drug by the body. For these compounds, increasing their aqueous solubility will improve their developability. Different strategies have been explored to increase the dissolution rate and solubility of poorly water-soluble drugs. Delivering the active pharmaceutical ingredient in the amorphous form is attractive due to the potentially large increases in drug solubility, dissolution rate, and bioavailability.<sup>3,4</sup> However, there is a risk of conversion of the amorphous form of a drug to the thermodynamically more stable crystalline counterpart during production and storage, reducing the performance benefit of the dosage form. To inhibit drug crystallization, a second

\* Corresponding author. Mailing address: Purdue University, Industrial and Physical Pharmacy, 575 Stadium Mall Drive, West Lafayette, IN 47907. E-mail: [lstaylor@purdue.edu](mailto:lstaylor@purdue.edu). Tel: +1-765-496-6614. Fax: +1-765-494-6545.

<sup>†</sup> Purdue University.

<sup>‡</sup> AstraZeneca Pharmaceuticals LP.

(1) Fahr, A.; Liu, X. *Expert Opin. Drug Delivery* **2007**, *4*, 403–416.

(2) Lipinski, C. A. *Am. Pharm. Rev.* **2002**, *5*, 82–85.

(3) Hancock, B. C.; Zografi, G. *J. Pharm. Sci.* **1997**, *86*, 1–12.

(4) Hancock, B. C.; Parks, M. *Pharm. Res.* **2000**, *17*, 397–404.

component (typically a water-soluble polymer) can be added,<sup>5</sup> forming what is commonly referred to as an amorphous solid dispersion.

Due to its hygroscopic nature, the addition of the polymer to form a solid dispersion can increase the amount of moisture sorbed compared to the pure amorphous drug alone. The absorption of water by an amorphous solid dispersion has many implications, and can negatively impact physical stability by increasing molecular mobility and promoting crystallization.<sup>6–8</sup> Recently, it has been shown that absorption of water by certain molecularly mixed amorphous solid dispersions composed of a hydrophobic drug and a hydrophilic polymer resulted in the formation of drug-rich and polymer-rich amorphous domains prior to drug crystallization.<sup>9–11</sup> This moisture-induced partial immiscibility, or amorphous-amorphous phase separation, has been reported for felodipine–poly(vinylpyrrolidone) (PVP),<sup>9,11,12</sup> nifedipine–PVP, pimozide–PVP, droperidol–PVP,<sup>10</sup> and griseofulvin–PVP.<sup>13</sup> However, this phenomenon was not observed for dispersions composed of indomethacin–PVP and ketoprofen–PVP.<sup>10</sup> It was also noted that the onset of drug crystallization for systems exhibiting moisture-induced phase separation occurred much sooner when compared to the systems that did not exhibit this behavior.<sup>10</sup> Given that moisture-induced changes in miscibility may be an underlying cause of reduced physical stability for certain solid dispersions upon exposure to accelerated stability testing conditions, it is of interest to better understand which systems are likely to be susceptible to this phenomenon.

One factor which seems to be important in determining whether sorption of water by an amorphous molecular level solid dispersion will result in the formation of amorphous drug-rich and polymer-rich domains prior to drug crystallization is the strength of drug–polymer interactions.<sup>10</sup> However, different polymers have different hygroscopicities in addition to being able to form different types of drug–polymer interactions.<sup>14</sup> Thus combining the same drug with different polymers at the same weight ratio may result in differing amounts of water being sorbed by the solid matrix under the same storage conditions.<sup>9</sup> The differing amounts of moisture sorbed will subsequently have different impacts on molecular mobility as well as the thermodynamics of the system.<sup>15</sup> The goal of this study was to test the hypothesis that solid dispersions prepared with less hygro-

scopic polymers will have a decreased susceptibility to moisture-induced changes in miscibility.

To assess the extent of drug–polymer mixing before and after exposure to moisture, model solid dispersion systems were studied primarily using mid-infrared (IR) spectroscopy. This technique was chosen due to its sensitivity to changes in local molecular chemical environments. By applying this technique, information on drug–polymer miscibility and drug crystallization can be obtained through analysis of intraspecies interactions (between drug molecules or polymer molecules) as well as interspecies interactions (between drug molecules and polymer molecules).<sup>10,16–18</sup> Disruption of interspecies interactions and the formation of intraspecies interactions following exposure to moisture indicate phase separation in the amorphous molecular level solid dispersion system, either as a result of crystallization of the drug or because of amorphous–amorphous phase separation.<sup>10</sup> In addition, the technique is relatively easy to apply, and characterization of the amorphous solid can be rapidly completed before drug crystallization commences. In addition to IR spectroscopy, differential scanning calorimetry (DSC) measurements were also conducted.

Three model polymers of differing hygroscopicities were chosen; the most hygroscopic was PVP, poly(vinylpyrrolidone-*co*-vinyl acetate) (PVPVA) had an intermediate hygroscopicity, and hypromellose acetate succinate (HPMCAS) was the least hygroscopic. Four model drugs, felodipine, quinidine, pimozide and indomethacin, were selected to encompass a range of chemistries and potential interactions with the polymers.

## Experimental Methods

Dichloromethane (ChromAR grade), chloroform (AR grade), and methanol (ACS reagent grade) were obtained from Mallinckrodt Baker, Inc., Phillipsburg, NJ, while ethanol (200 proof) was obtained from PHARMCO-AAPER, Brookfield, CT. Felodipine was a generous gift from Astra-Zeneca, Södertälje, Sweden. PVP K29-32, pimozide, quinidine, and indomethacin were purchased from Sigma-Aldrich Co., St. Louis, MO. HPMCAS (AQOAT AS-MF) was obtained from ShinEtsu Chemical Co., Niigata, Japan, while PVPVA (Kollidon VA 64) was a gift from BASF Chemical Company, Ludwigshafen, Germany. Unless otherwise noted, experiments were conducted at room temperature (22–25 °C).

**Infrared Spectroscopy.** Binary mixtures of the model drug and polymer at different weight ratios were dissolved in a common solvent. For felodipine- and quinidine-containing systems as well as indomethacin–HPMCAS, the solvent

(5) Ford, J. L. *Pharm. Acta Helv.* **1986**, *61*, 69–88.

(6) Shamblyn, S. L.; Zografi, G. *Pharm. Res.* **1999**, *16*, 1119–1124.

(7) Saleki-Gerhardt, A.; Zografi, G. *Pharm. Res.* **1994**, *11*, 1166–1173.

(8) Andronis, V.; Zografi, G. *Pharm. Res.* **1998**, *15*, 835–842.

(9) Konno, H.; Taylor, L. S. *Pharm. Res.* **2008**, *25*, 969–978.

(10) Rumondor, A. C. F.; Marsac, P. J.; Stanford, L. A.; Taylor, L. S. *Mol. Pharmaceutics* **2009**, *6* (5), 1492–1505.

(11) Marsac, P. J.; Rumondor, A. C. F.; Nivens, D. E.; Kestur, U. S.; Stanciu, L.; Taylor, L. S. *J. Pharm. Sci.* **2010**, *99* (1), 169–185.

(12) Marsac, P. J. PhD Thesis, Purdue University, West Lafayette, 2007.

(13) Vasanthavada, M.; Tong, W. Q.; Joshi, Y.; Kislalioglu, M. S. *Pharm. Res.* **2005**, *22*, 440–448.

(14) Konno, H.; Taylor, L. S. *J. Pharm. Sci.* **2006**, *95*, 2692–2705.

(15) Marsac, P. J.; Konno, H.; Rumondor, A. C. F.; Taylor, L. S. *Pharm. Res.* **2008**, *25*, 647–656.

(16) Taylor, L. S.; Zografi, G. *Pharm. Res.* **1997**, *14*, 1691–1698.

(17) Wang, L. A.; Cui, F. D.; Hayase, T.; Sunada, H. *Chem. Pharm. Bull.* **2005**, *53*, 1240–1245.

(18) Marsac, P. J.; Konno, H.; Taylor, L. S. *Pharm. Res.* **2006**, *23*, 2306–2316.

used was a 1:1 w/w mixture of dichloromethane and ethanol, while for indomethacin–PVPVA, the solvent was pure ethanol. Chloroform was used for pimozide–PVPVA, while a 1:1 v/v mixture of methanol and chloroform was used for pimozide–HPMCAS. All mixtures were visually inspected to confirm that the solids were fully dissolved before further use, and that the systems formed uniform one-phase solutions.

One to two drops of the solution was then placed on ZnS or KRS-5 IR substrates, which were immediately rotated on a KW-4A two-stage spin coater (Chemat Technology, Northridge, CA) at approximately 500/2500 rpm for 18 and 30 s respectively (the exact speed and time were individually adjusted so that the absorbance intensity of the spectral region of interest was between 0.4 and 1.0). Immediately after spin-coating, the substrates were transferred onto a hot plate set to 90 °C for at least a minute to remove any residual solvents. IR spectra of the resulting thin films were obtained in absorbance mode using a Bio-Rad FTS 6000 spectrophotometer (Bio-Rad Laboratories, Hercules, CA) equipped with globar infrared source, KBr beamsplitter, and DTGS detector. The scan range was set from 500 to 4000  $\text{cm}^{-1}$  with 4  $\text{cm}^{-1}$  resolution, and 128 scans were coadded. During measurement, the sample and the sample compartment of the spectrophotometer were flushed with dry air to minimize interference from absorbed and gas-phase moisture.

After the initial IR spectra were obtained, the samples were stored in desiccators kept at 54% RH using a saturated salt solution of  $\text{Mg}(\text{NO}_3)_2$ . After at least one day, the solid dispersion samples were removed from the desiccators, rigorously dried by flushing with dry air (RH < 10%) until no changes in the OH spectral region were observed, and reanalyzed by IR spectroscopy. The samples were dried before analysis so that absorbed moisture would not mask changes in the extent of the drug–polymer interactions. This procedure was repeated for the same samples using desiccators maintained at 75% RH (saturated NaCl solution), 84% RH (saturated KCl solution), and 94% RH (saturated  $\text{KNO}_3$  solution). RH conditions were chosen based on previous results.<sup>10,11</sup> Reference spectra of the amorphous form of the drugs and pure polymers were collected using the aforementioned spin-coating technique, while reference spectra of the crystalline drugs were obtained using a Golden Gate MkII attenuated total reflectance unit with diamond top-plate (Specac Inc., Woodstock, GA).

**Preparation of Bulk Amorphous Solid Dispersion Samples.** To produce bulk powder amorphous solid dispersion samples, the drug and the polymer were first dissolved using the same common solvents as used in the preparation of IR samples. The solvent was then removed using a rotary evaporator apparatus (Brinkman Instruments, Westbury, NY), and the samples were placed under vacuum for at least 12 h to remove any residual solvents. The resultant solid was gently ground using a mortar and pestle in a glovebox flushed with dry air (RH < 10%), and stored under vacuum prior to use.

**Differential Scanning Calorimetry (DSC).** Glass transition temperatures ( $T_g$ s) for the pure drugs and polymers were

determined using DSC. For these measurements, the powder samples were placed in TZero aluminum pans (TA Instruments, New Castle, DE), heated at 20 °C/min to 10 °C above the  $T_m$  of the drug or the  $T_g$  of the polymer, held isothermally for 60 s, cooled at >20 °C/min to –40 °C, and then reheated to the same upper temperature at 20 °C/min. The cycle was repeated three times to ensure the precision of  $T_g$  measured. For pure polymers, pans with pinholes were used, so that sorbed moisture could be released during the first heating cycle. Results from the second and third heating cycles were then used to determine the  $T_g$ s of the pure polymers.

DSC measurements were also carried out on the solid dispersion systems. For these measurements, bulk solid dispersion powder was placed in two identical TZero aluminum pans (TA Instruments, New Castle, DE). DSC measurement was immediately performed on the first sample by heating at 20 °C/min to 10 °C above the  $T_m$  of the drug or the  $T_g$  of the pure polymer (whichever was higher), holding the sample at that temperature for 60 s, cooling it at >20 °C/min to –40 °C, and then reheating it at 20 °C/min to the same upper temperature. The heating cycle was repeated three times. The second sample was exposed to 25 °C/94% RH using an SGA-100 symmetrical gravimetric analyzer instrument (VTI Corporation, Hialeah, FL) at a flow rate of 200 mL/min for 24 h, followed by exposure to dry air (RH < 3% at 25 °C) until a plateau in the weight loss was observed (approximately 48 h). After the drying step, the pans were hermetically sealed, and the samples were analyzed using the same heating procedure as the first sample.

A Q2000 DSC (TA Instruments, New Castle, DE) equipped with a refrigeration cooling system (RCS) attachment was used to perform all DSC measurements. The enthalpic response was calibrated using indium, while the temperature scale was calibrated using indium and tin. Data analyses for all measurements were performed using Universal Analysis 2000 software v. 4.1D (TA Instruments, New Castle, DE).

**Moisture Sorbed by Solid Dispersions at 25 °C/85% Relative Humidity.** The amount of moisture sorbed at 25 °C and 85% RH was measured using the symmetrical gravimetric analyzer instrument for four solid dispersion systems containing 25% polymer (dry weight basis). For these measurements, approximately 10–15 mg of the bulk solid dispersion sample was loaded into the gravimetric analyzer, flushed with dry air (RH < 2%) for 3 h at 25 °C, and then exposed to 85% RH. The amount of moisture sorbed by the various systems was estimated from a plot of weight gain versus time, and was taken as the value where a plateau was initially observed.

## Results

**Miscibility of Drug–Polymer Systems in the Absence of Moisture.** IR spectroscopy and DSC were used to interrogate drug–polymer miscibility of the various model solid dispersion systems. In IR spectroscopy, peaks arise due

to absorption of IR radiation by the chemical moieties resonating at certain frequencies. However, the resonant frequencies of the various chemical moieties are affected by the local chemical environments of the molecules. In the absence of any mixing (i.e., a completely immiscible solid dispersion system), the local chemical environments of the drug and the polymer molecules are similar to their environments in the pure systems. Thus the IR spectra for such amorphous solid dispersions would be very similar to the IR spectra of a physical mixture containing the amorphous drug and the polymer at the same weight ratio. In completely miscible systems, where the drug and the polymers are mixed at the molecular level, changes in the chemical environments due to interspecies interactions result in changes in IR peak locations or relative intensity that can not be attributed solely to changes in the composition of the samples. As a result, the IR spectra of miscible solid dispersions possess features that are different from the spectra of physical mixtures of an amorphous drug and a polymer. Since these differences are caused by drug–polymer interactions, they are most easily identified by observing IR peaks assigned to the moieties responsible for the interactions, for example the  $-\text{NH}$ ,  $-\text{OH}$ , and carbonyl moieties in the drug and polymer molecules that can act as hydrogen bond donors or acceptors. An additional advantage of IR spectroscopy is that it can also be used to identify phase separation from amorphous solid dispersions in the form of drug crystallization.<sup>16,19,20</sup>

For all dry solid dispersions studied, analysis of the IR spectra collected immediately after sample preparation showed clear evidence for drug–polymer interactions, providing support for drug–polymer mixing at the molecular level. The IR peak assignments for the specific functional groups responsible for the drug–polymer interactions are listed in Table 1, and the chemical structures of the model compounds are shown in Figure 1. Drug–polymer interactions have been reported previously for felodipine–HPMCAS,<sup>9,14</sup> thus the results of this study serve to confirm that this system can form miscible solid dispersions. IR results for other model systems studied indicate that they can also form molecular level dispersions as evidenced by the presence of drug–polymer specific interactions.

In DSC measurements of amorphous substances, an inflection in the heat flow vs temperature curve would indicate a glass transition event, and the temperature of this event is called the calorimetric glass transition temperature ( $T_g$ ). In a two-component amorphous systems with limited miscibility, the existence of two different amorphous phases can be verified by the presence of more than one  $T_g$ , for example as reported for PVP–dextran and PVP–PVPVA,<sup>21</sup> itraconazole–Eudragit,<sup>22</sup> and citric acid–indomethacin.<sup>23</sup>

However, if the two components in the mixture are mixed at the molecular level, then only one  $T_g$  can be detected. In such cases, the  $T_g$  of the mixture usually occurs between the  $T_g$ s of the pure components. The presence of a single  $T_g$  has been previously reported for felodipine–HPMCAS dispersions.<sup>14</sup> In this study, a single  $T_g$  was recorded for this system as well as for all the other model systems studied immediately after production (see Table 3). As is apparent from Tables 2 and 3, the solid dispersions had  $T_g$  values that were intermediate to the  $T_g$  values of the pure components. Together with the IR data, these results support the conclusion that, in the absence of water, all drug–polymer model systems studied were mixed at the molecular level, forming one-phase amorphous solid dispersions.

**Miscibility of Solid Dispersions Following Exposure to Moisture.** Once drug–polymer mixing at the molecular level was confirmed, the samples were exposed to moisture to see if drug–polymer miscibility would be adversely affected. If it is, then the intensity of IR peaks assigned to drug–polymer specific interactions should be reduced relative to those arising from drug–drug or polymer–polymer interactions. The extent of the reduction is expected to be commensurate with the extent of drug–polymer demixing induced by the absorption of water. If the extent of drug–polymer demixing is severe, then two amorphous phases, a highly drug-rich and a highly polymer-rich phase, would be produced. In such cases, contributions from the IR peaks assigned to drug–polymer specific interactions would be minimal, and the resulting spectra would be similar to those of physical mixtures composed of the pure amorphous drug and pure polymer. The DSC thermograms of such systems are expected to show two  $T_g$ s close to the  $T_g$ s of the pure drug and the pure polymer, assuming remixing during the DSC measurement is minimal. On the other hand, if the extent of moisture-induced drug–polymer demixing is less extensive, then two amorphous phases would still be produced, one richer in polymer and the other richer in drug. However, the drug-rich phase would still contain a significant concentration of polymer, and the polymer-rich phase would still contain a significant concentration of the drug. As a result, contributions from the IR peaks assigned to drug–polymer specific interactions would still be significant, and the resulting IR spectra of the solid dispersion sample would be similar to a combination of two solid dispersions with different drug–polymer weight ratios. The DSC thermograms of such systems are again expected to show two  $T_g$ s, but they will be different from the  $T_g$ s of the pure drug and the pure polymer.

In making these comparisons, it is important to eliminate interference from water, both for IR and for DSC samples. Therefore, the systems described below are binary systems from which water has been removed by flushing with dry air.

(19) Chan, K. L. A.; Fleming, O. S.; Kazarian, S. G.; Vassou, D.; Chrysoskos, G. D.; Gionis, V. J. *Raman Spectrosc.* **2004**, *35*, 353–359.

(20) He, X. R.; Griesser, U. J.; Stowell, J. G.; Borchardt, T. B.; Byrn, S. R. *J. Pharm. Sci.* **2001**, *90*, 371–388.

(21) Shamblyn, S. L.; Taylor, L. S.; Zografi, G. *J. Pharm. Sci.* **1998**, *87*, 694–701.

(22) Six, K.; Murphy, J.; Weuts, I.; Craig, D. Q. M.; Verreck, G.; Peeters, J.; Brewster, M.; Van den Mooter, G. *Pharm. Res.* **2003**, *20*, 135–138.

(23) Lu, Q.; Zografi, G. *Pharm. Res.* **1998**, *15*, 1202–1206.



**Table 1.** Infrared Spectroscopy Peak Assignments for Systems Studied

systems	wavenumber <sup>a</sup> (cm <sup>-1</sup> )	assignment
poly(vinyl pyrrolidone)/PVP	1681	$\nu$ C=O, non H-bonded
poly(vinylpyrrolidone-co-vinyl acetate)/PVPVA	1683	$\nu$ C=O of (vinylpyrrolidone), non H-bonded
	1737	$\nu$ C=O of (vinyl acetate), non H-bonded
hypromellose acetate succinate (HPMCAS)	1742	ester carbonyl
	1714 <sup>sh</sup>	acidic carbonyl
Pimozide-Containing Systems		
amorphous pimozide	1696	$\nu$ C=O in dimers
	1709 <sup>sh</sup>	$\nu$ C=O, non H-bonded
pimozide–PVPVA solid dispersion	1661 <sup>sh,w</sup>	$\nu$ C=O of (vinylpyrrolidone) when H-bonded to quinidine
	1709	$\nu$ C=O of pimozide, non H-bonded
	1736	$\nu$ C=O of (vinyl acetate), non H-bonded
pimozide–HPMCAS solid dispersion	1741	HPMCAS ester
	1704 (broad)	free pimozide (1709) overlapping with $\nu$ C=O in dimers
Indomethacin-Containing Systems		
amorphous indomethacin	1685	benzoyl C=O
	1710	acid C=O in dimers
	1735 <sup>sh</sup>	non H-bonded acid C=O
indomethacin–PVPVA solid dispersion	1640	$\nu$ C=O of PVP when H-bonded to indomethacin
	1683	acid C=O, non H-bonded
	1734	$\nu$ C=O of (vinyl acetate), non H-bonded
indomethacin–HPMCAS solid dispersion	1685	benzoyl C=O
	1712	H-bonded acid C=O
	1740	ester carbonyl from HPMCAS
Felodipine-Containing Systems		
amorphous felodipine	3418	$\nu$ NH, non H-bonded
	3341	$\nu$ NH, H-bonded to drug molecules
	1701	free carbonyl drug
	1682	h-bonded carbonyl drug
felodipine–PVPVA solid dispersion	3297	$\nu$ NH of felodipine when H-bonded to PVPVA
	3341	$\nu$ NH of felodipine when H-bonded to felodipine
felodipine–HPMCAS solid dispersion	1739	ester carbonyl of HPMCAS
	1683	$\nu$ C=O felodipine, H-bonded to other drug molecules
	1701	$\nu$ C=O felodipine, non H-bonded
	3346	$\nu$ NH, H-bonded to polymer molecules
Quinidine-Containing Systems		
quinidine–PVP solid dispersion	1662	$\nu$ C=O of PVP when H-bonded to quinidine
	1681	$\nu$ C=O of PVP, non H-bonded
quinidine–PVPVA solid dispersion	1665	$\nu$ C=O of (vinylpyrrolidone) when H-bonded to quinidine
	1683	$\nu$ C=O of (vinylpyrrolidone), non H-bonded
	1737	$\nu$ C=O of (vinyl acetate), non H-bonded
quinidine–HPMCAS solid dispersion	1745	Ester carbonyl of HPMCAS

<sup>a</sup> sh = shoulder, w = weak.

**Systems Exhibiting Moisture-Induced Amorphous–Amorphous Phase Separation.** IR spectra showing the regions of interest for felodipine–PVPVA, quinidine–PVP, quinidine–PVPVA, pimozide–PVPVA, and pimozide–HPMCAS samples before and after exposure to moisture are shown in Figures 2a–6a. The corresponding DSC thermograms for these systems are shown in Figures 2b–6b. The results suggest that, for these systems, exposure to moisture during storage at the specified relative humidity (RH) resulted in the formation of drug-rich and polymer-rich amorphous phases.

For felodipine–PVPVA, the NH region of the IR spectra is very useful to study drug–polymer specific interactions. Drug–polymer hydrogen bonding resulted in a shift of the peak assigned to the NH moiety of the drug from 3341 cm<sup>-1</sup> to 3297 cm<sup>-1</sup>. When the sample was stored at increasing RH, the relative intensity of the peak centered at 3341 cm<sup>-1</sup> increased (see Figure 2a), suggesting the formation of drug–drug specific interactions at the expense of drug–polymer specific interactions. The DSC thermograms show that following storage at 94% RH and subsequent drying, two  $T_g$ s were recorded between

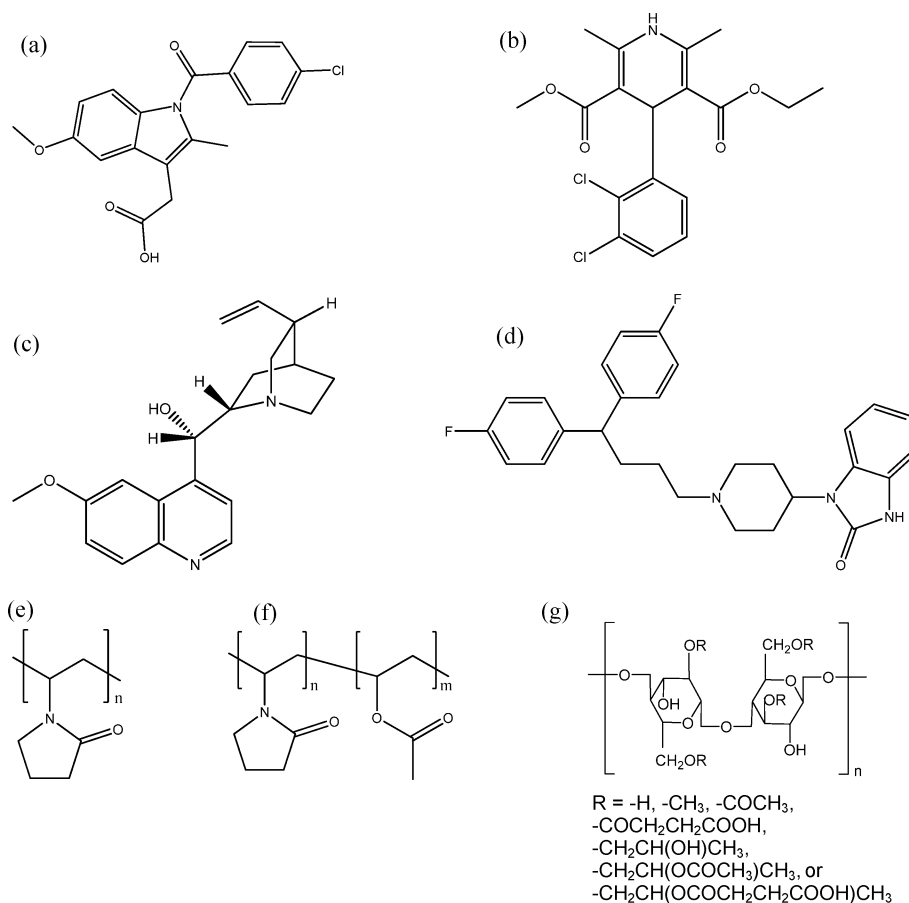


**Figure 1.** Chemical structures of (a) indomethacin, (b) felodipine, (c) quinidine, (d) pimozone, and the repeating units of (e) PVP, (f) PVPVA, and (g) HPMCAS.

**Table 2.** Selected Physical Properties of the Model Drugs Used

	MW (g/mol)	aq solubility (g/L)	calcd log <i>P</i> <sup>c</sup>	<i>T</i> <sub>m,onset</sub> (°C)	<i>T</i> <sub>g,midpoint</sub> (°C)	Δ <i>C</i> <sub>p</sub> [J/(g °C)]
felodipine	384.26	2.7 × 10 <sup>-3</sup> (25 °C) <sup>a</sup>	2.24	143.4	47	0.346
quinidine	324.42	1.4 × 10 <sup>-1</sup> (25 °C) <sup>b</sup>	2.48	170.6	61	0.592
pimozone	461.56	2.9 × 10 <sup>-3</sup> (30 °C) <sup>b</sup>	5.34	217.8	62	0.404
indomethacin	357.81	4–14 × 10 <sup>-3</sup> (25 °C) <sup>b</sup>	3.58	159.1	48	0.415
PVP					166	0.391
PVPVA					107	0.387
HPMCAS					121	0.288

<sup>a</sup> As reported in ref 15. <sup>b</sup> As reported in ref 35. <sup>c</sup> As reported in ChemBioDraw Ultra v 11.0, CambridgeSoft Corp., Cambridge, MA.

the *T*<sub>g</sub>s of the pure drugs and the pure polymer, identifying the presence of more than one amorphous phase (see Figure 2b, Table 3).

Since quinidine does not have a carbonyl moiety in its structure, this region of the IR spectra is amenable to studying drug–polymer interactions in quinidine-containing ASD samples by analyzing peaks attributed to the carbonyl moieties of the polymers. Quinidine contains a hydroxyl group that can potentially hydrogen bond with hydrogen bond acceptor groups on the polymer. Only one peak, assigned to the free carbonyl moiety of PVP (centered at 1681 cm<sup>-1</sup>), is observed in the absence of the drug (see Figure 3a). In solid dispersion samples, a shoulder developed at 1662 cm<sup>-1</sup>. This peak is assigned to the carbonyl peak of PVP when hydrogen bonded to the OH moiety of the drug. Following storage at

54% RH, the peak centered at 1662 cm<sup>-1</sup> decreased in relative intensity. The trend was continued as the storage RH was increased and, as shown in Figure 3a, following storage at 84% RH, this shoulder is virtually eliminated. These results again suggested disruption in drug–polymer specific interactions following exposure to moisture. DSC thermograms of the same system following storage at 94% RH for 24 h and subsequent drying also shows two *T*<sub>g</sub>s recorded between the *T*<sub>g</sub>s of the pure amorphous components (see Figure 3b, Table 3).

For the quinidine–PVPVA model system, three peaks were observed between 1650 and 1800 cm<sup>-1</sup> (see Figure 4a). The peak centered at 1665 cm<sup>-1</sup> is absent in the spectra of pure polymer or pure amorphous drug, and is assigned to the carbonyl peak of the vinylpyrrolidone moiety of PVPVA

**Table 3.** DSC Results of Solid Dispersion Model Systems

system	before exposure to moisture		after exposure to moisture and drying			
	$T_g$ (°C)	$\Delta C_p$ [J/(g °C)]	$T_{g,1}$ (°C)	$\Delta C_{p,1}$ [J/(g °C)]	$T_{g,2}$ (°C)	$\Delta C_{p,2}$ [J/(g °C)]
felodipine–50% PVPVA	77	0.353	64	0.271	77	0.116
quinidine–50% PVP	70	0.367	63	0.179	81	0.261
quinidine–50% PVPVA	69	0.411	62	0.298	76	0.139
pimozide–50% PVPVA	83	0.353	59	0.214	97	0.171
pimozide–50% HPMCAS	78	0.431	65	0.371	79	0.151
felodipine–50% HPMCAS <sup>a</sup>	56	0.379	56	0.278		
quinidine–50% HPMCAS <sup>a</sup>	68	0.436	65	0.422		
indomethacin–50% PVPVA <sup>a</sup>	63	0.420	67	0.543		
indomethacin–50% HPMCAS <sup>a</sup>	49	0.431	54	0.397		

<sup>a</sup> For the last four systems listed, only one glass transition event was recorded following exposure of the solid dispersion samples to moisture and subsequent drying.

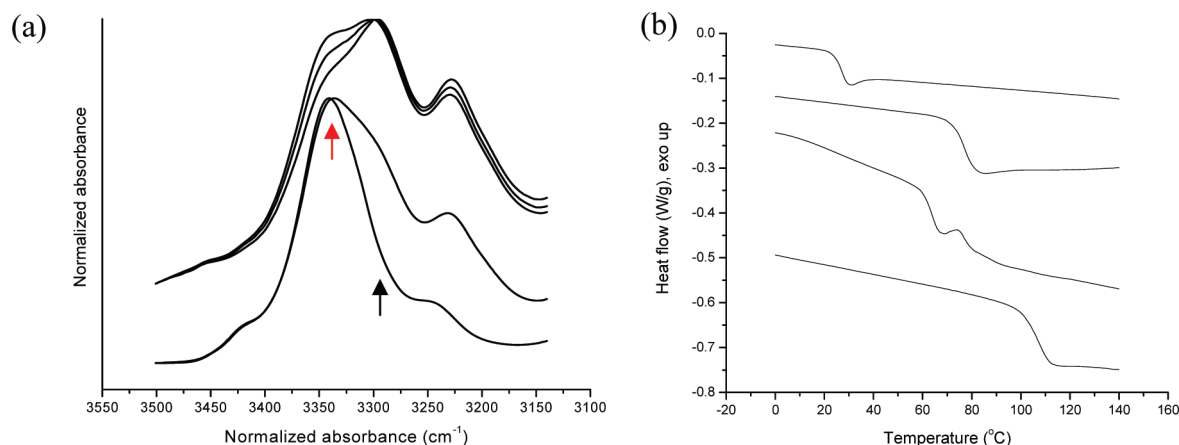


**Figure 2.** (a) IR spectra of the NH region of (from top to bottom) solid dispersion sample containing felodipine and 50% PVPVA after 1-day storage at 84% RH, after 1-day storage at 54% RH, immediately after preparation, solid dispersion sample containing felodipine and 50% PVP after 1-day storage at 84% RH, and amorphous felodipine. The black arrow indicates a relative decrease in drug–polymer interactions while the red arrow indicates a relative increase in drug–drug interactions in the amorphous form following exposure to moisture. Pure PVP and PVPVA do not have significant IR absorption in this region. (b) DSC thermograms of (from top to bottom) amorphous felodipine, solid dispersion sample containing felodipine and 50% PVPVA, identical solid dispersion sample following 1-day storage at 94% RH and subsequent drying, and pure PVPVA.

when hydrogen bonded to the OH moiety of the drug molecules. Following storage at increasing RH, the relative intensity of this peak decreased slightly, indicating some disruption of drug–polymer hydrogen bonding. Interestingly, the extent of this decrease was much less than that observed for the quinidine–PVP dispersion. From Figure 4b, it can be seen that the system, which exhibited only a single  $T_g$  immediately after formation, showed two  $T_g$ s following storage at 94% RH and subsequent drying, indicating the presence of two different amorphous phases in the samples.

For pimozide–PVPVA, four peaks can be observed in the carbonyl region, two of which result from drug–polymer specific interactions. The peak centered at  $1661\text{ cm}^{-1}$  (appearing as a weak shoulder) is assigned to the vinylpyrrolidone moiety of the polymer when hydrogen bonded to drug molecules, and the peak centered at  $1709\text{ cm}^{-1}$  is assigned to the free carbonyl moiety of pimozide, which is detectable when drug–drug hydrogen bonding is disrupted<sup>10</sup> following the formation of drug–polymer interactions. Exposure of pimozide–PVPVA samples to increasing RH

resulted in intensity reduction for these two peaks, suggesting disruption of drug–polymer specific interactions in favor of drug–drug interactions in the amorphous form. In addition, DSC results clearly indicated the presence of two  $T_g$ s, followed by recrystallization and subsequent melting of pimozide upon further heating of the sample (see Figure 6b).

The presence of overlapping peaks in the IR spectra of pimozide–HPMCAS samples cause difficulties in spectral interpretation. Close examination of the spectra (data not shown) revealed the presence of a weak shoulder centered at  $1711\text{ cm}^{-1}$  in the sample containing 10% polymer, which increased in relative intensity for the sample containing 30% polymer, and became a broad peak centered at  $1704\text{ cm}^{-1}$  for the sample containing 50% polymer. This peak is assigned to the free carbonyl moiety of pimozide, partially overlapping with the carbonyl peak of pimozide when hydrogen-bonded to other drug molecules in the amorphous form (centered at  $1696\text{ cm}^{-1}$ ).

When the sample containing 50% polymer was exposed to increasing RH, the broad peak centered at  $1704\text{ cm}^{-1}$  split

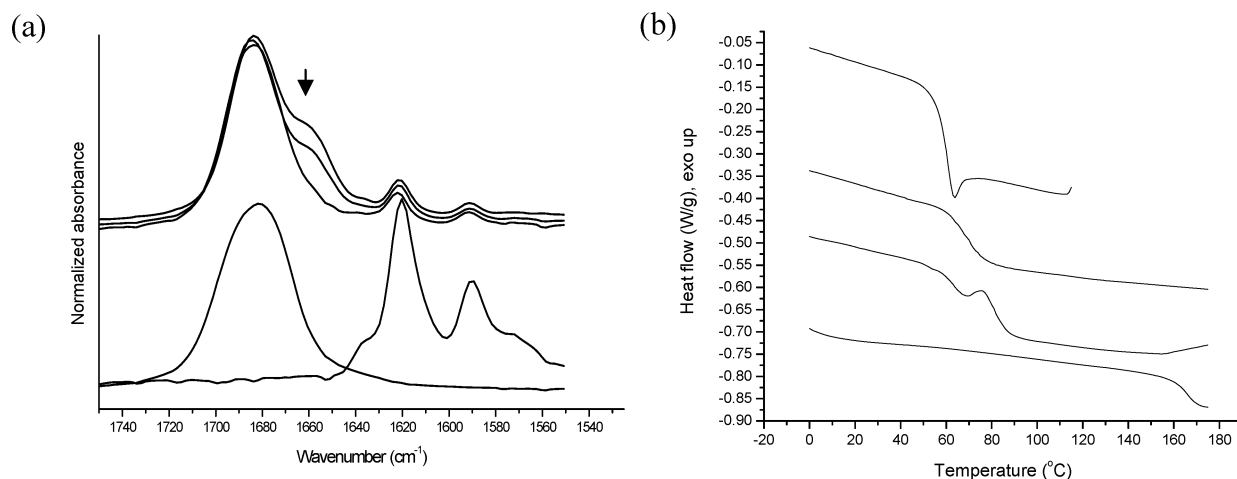


**Figure 3.** (a) IR spectra of the carbonyl region of (top to bottom) solid dispersion sample containing quinidine and 50% PVP immediately after preparation, the same sample after 1-day storage at 54% RH and at 84% RH, pure amorphous quinidine (spectrum with peaks between 1640–1660  $\text{cm}^{-1}$ ), and pure PVP (spectrum with peak at 1680  $\text{cm}^{-1}$ ). The arrow indicates a decrease in drug–polymer interactions following exposure to moisture. (b) DSC thermograms of (from top to bottom) amorphous quinidine, solid dispersion sample containing quinidine and 50% PVP, identical solid dispersion sample following 1-day storage at 94% RH and subsequent drying, and pure PVP.

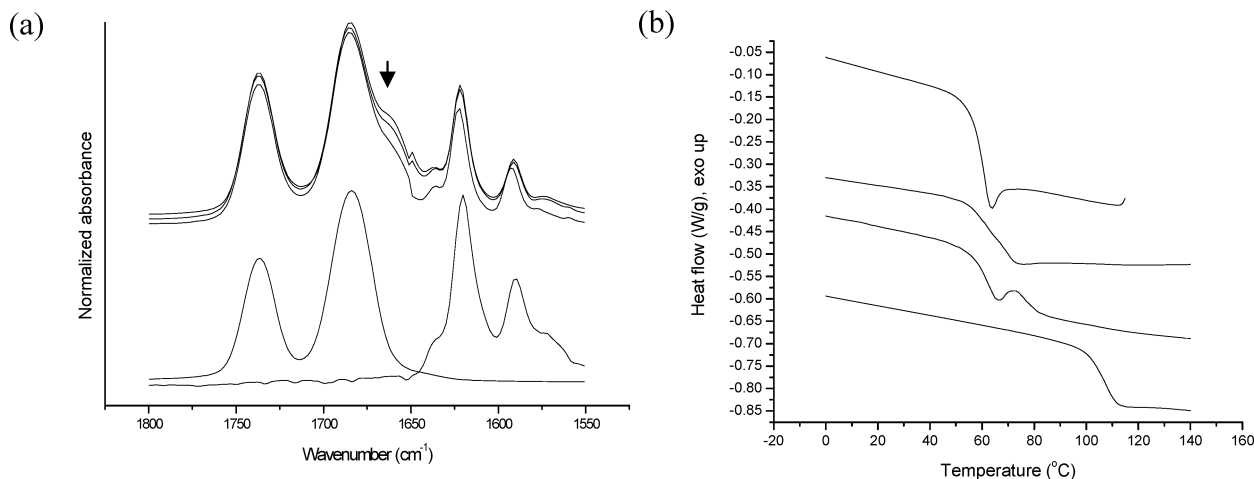


**Figure 4.** (a) IR spectra of the carbonyl region of (from top to bottom) solid dispersion sample containing quinidine and 50% PVP immediately after preparation, the same sample after 1-day storage at 84, the same sample after 1-day storage at 94% RH, pure quinidine, and pure PVP. The arrow indicates a decrease in drug–polymer interactions following exposure to moisture. (b) DSC thermograms of (from top to bottom) amorphous quinidine, solid dispersion sample containing quinidine and 50% PVP, identical solid dispersion sample following 1-day storage at 94% RH and subsequent drying, and pure PVP.

into a peak centered at 1709  $\text{cm}^{-1}$  and a shoulder centered at 1698  $\text{cm}^{-1}$ . Development of the shoulder centered at 1698  $\text{cm}^{-1}$  is attributable to an increase in the relative abundance of drug–drug hydrogen bonding, resulting in a clearer presence of the peak (shifted to a higher wavenumber due to peak overlap). However, the intensity of the peak centered at 1698  $\text{cm}^{-1}$  is still lower compared to the peak centered at 1709  $\text{cm}^{-1}$ , indicating a significant presence of the peak assigned to drug–polymer hydrogen bonding. While specific locations and features of the peaks are difficult to discern due to relatively small changes as well as significant overlaps, these changes suggest molecular level compositional changes consistent with the formation of drug-rich and polymer-rich

regions with still significant amounts of the other component present in each amorphous phase.

This conclusion is better supported by the DSC results. Following storage at 94% RH and subsequent drying, two  $T_g$ s were again recorded. However, the  $T_g$ s recorded are very close to each other as well as the  $T_g$  of the dry solid dispersion (see Figure 6b).

For the model systems discussed above, similar trends (to differing extents) were observed with solid dispersions containing 30 and 70% polymer, while the absence of the crystalline form of the drug was verified visually as well as by examining other regions of the IR spectra to confirm that peaks characteristic of the crystalline form were absent (e.g.,



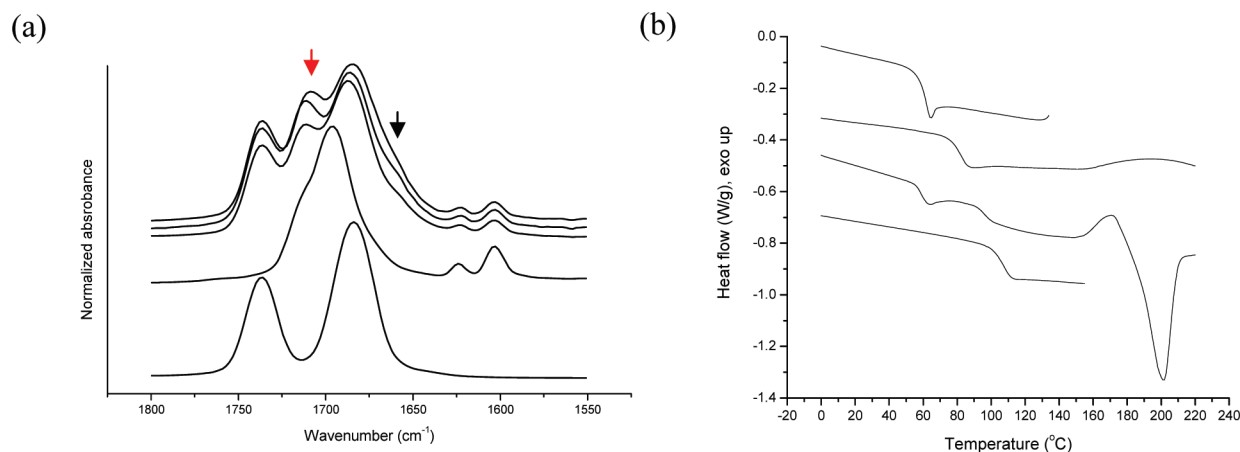


**Figure 5.** (a) IR spectra of the carbonyl region of (from top to bottom) solid dispersion sample containing pimoziide and 50% PVPVA immediately after preparation, the same sample after 1-day storage at 54% RH, the same sample after 1-day storage at 84% RH, pure amorphous pimoziide, and pure PVPVA. The black arrow indicates a relative decrease in drug–polymer interactions while the red arrow indicates a relative increase in drug–drug interactions in the amorphous form following exposure to moisture. (b) DSC thermograms of (from top to bottom) amorphous pimoziide, solid dispersion sample containing pimoziide and 50% PVPVA, identical solid dispersion sample following 1-day storage at 94% RH and subsequent drying, and pure PVPVA.

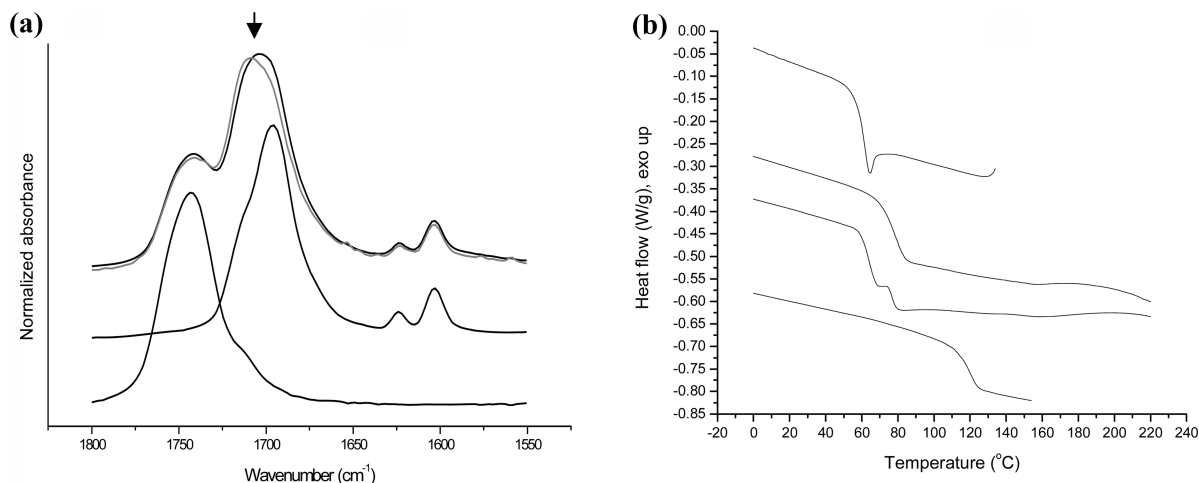


**Figure 6.** (a) IR spectra of the carbonyl region of (from top to bottom) solid dispersion sample containing pimoziide and 50% HPMCAS immediately after preparation, the same sample after 1-day storage at 94% RH (colored gray), pure amorphous pimoziide, and pure HPMCAS. The arrow indicates a decrease in drug–polymer interaction characteristics following exposure to moisture. (b) DSC thermograms of (from top to bottom) amorphous pimoziide, solid dispersion sample containing pimoziide and 50% HPMCAS, identical solid dispersion sample following 1-day storage at 94% RH and subsequent drying, and pure HPMCAS.

the OH region for quinidine-containing systems). For samples containing 10 and 90% polymer, moisture-induced drug–polymer demixing could not be completely verified nor disqualified due to the sensitivity limitations of the methods used.

**Systems Not Exhibiting Moisture-Induced Amorphous–Amorphous Phase Separation.** If moisture-induced amorphous–amorphous phase separation does not occur, then no significant change is expected in the IR spectra of samples following exposure to moisture and subsequent drying. Such a result would indicate that drug–polymer interactions were undisturbed in the presence of moisture, and that the sample remained a single amorphous phase. DSC measurements of these samples are expected to show only one only glass

transition event at approximately the same temperature as for the dry samples.

The spectra of the carbonyl regions of felodipine–HPMCAS, indomethacin–PVPVA, indomethacin–HPMCAS, and quinidine–HPMCAS samples are shown in Figures 7a–10a. For these systems, the results show that, following storage at room temperature and at various RHs up to 94%, no changes were observed in the IR regions of interest.

In indomethacin–PVPVA, the peak centered at  $1640\text{ cm}^{-1}$  (assigned to the carbonyl moiety in vinylpyrrolidone when hydrogen-bonded to the drug molecules) and the peak centered at  $1683\text{ cm}^{-1}$  (free vinylpyrrolidone carbonyl peak

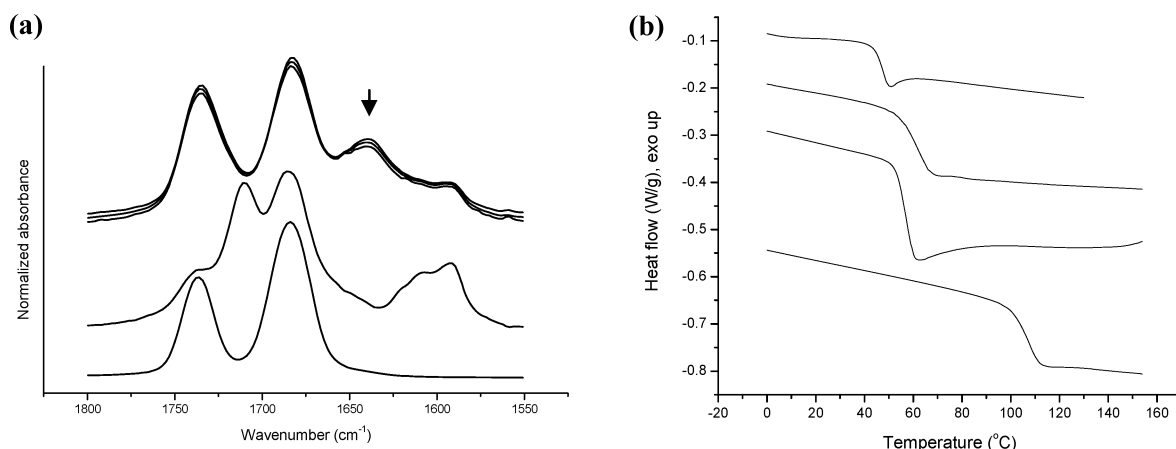


**Figure 7.** (a) IR spectra of the carbonyl region of (from top to bottom) solid dispersion samples containing indomethacin and 50% PVPVA immediately after preparation, the same sample after 1-day storage at 75% RH, and the same sample after 7-day storage at 94% RH (7 days), pure amorphous indomethacin, and pure PVPVA. The arrow shows a carbonyl peak arising as a result of drug–polymer hydrogen bonding that was unaffected by exposure to moisture. (b) DSC thermograms of (from top to bottom) amorphous indomethacin, solid dispersion sample containing indomethacin and 50% PVPVA, identical solid dispersion sample following 1-day storage at 94% RH and subsequent drying, and pure PVPVA.

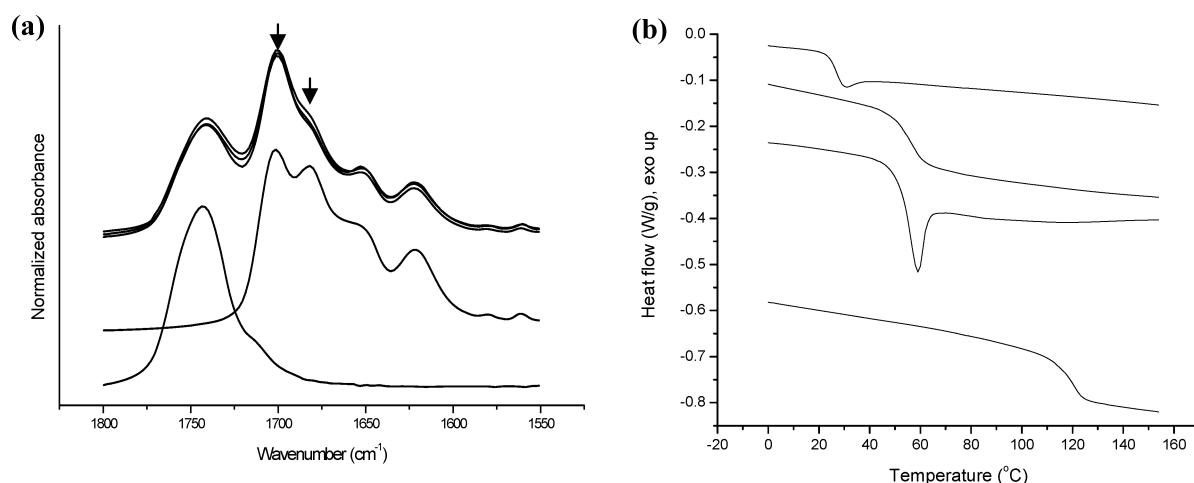


**Figure 8.** (a) IR spectra of the carbonyl region of (from top to bottom) solid dispersion samples containing felodipine and 50% HPMCAS immediately after preparation, the same sample after 1-day storage at 75% RH, the same sample after 2-day storage at 94% RH, pure amorphous felodipine, and pure HPMCAS. The relative intensity of the two peaks indicated by arrows were unaffected by exposure to moisture (see text for assignments). (b) DSC thermograms of (from top to bottom) amorphous felodipine, solid dispersion sample containing felodipine and 50% HPMCAS, identical solid dispersion sample following 1-day storage at 94% RH and subsequent drying, and pure HPMCAS.

overlapping with the benzoyl carbonyl of amorphous indomethacin) were both present at the same relative intensity (see Figure 7a). For felodipine–HPMCAS, the peaks centered at 1701 and 1683  $\text{cm}^{-1}$  (assigned to free carbonyl of felodipine and the same moiety when hydrogen bonded to other drug molecules respectively) were always present at the same relative intensity (see Figure 8a).

For indomethacin, the peak centered at 1712  $\text{cm}^{-1}$  is assigned to asymmetric  $\nu\text{C}=\text{O}$  of the cyclic dimer of indomethacin, while the peak centered at 1685  $\text{cm}^{-1}$  is assigned to the benzoyl carbonyl of indomethacin in the

amorphous form (see Table 1). In the indomethacin–HPMCAS solid dispersion, a decrease in the intensity of the peak centered at 1712  $\text{cm}^{-1}$  was observed when compared to the peak centered at 1685  $\text{cm}^{-1}$ , signifying disruption in drug–drug specific interactions in the presence of the polymer. Following storage at increasing RH and subsequent drying, the ratio of these two peaks remained constant, indicating persistent disruption in drug–drug hydrogen bonding due to drug–polymer specific interactions.

For quinidine–HPMCAS, the weak shoulder at 1714  $\text{cm}^{-1}$  (assigned to the acidic carbonyl of HPMCAS) was absent

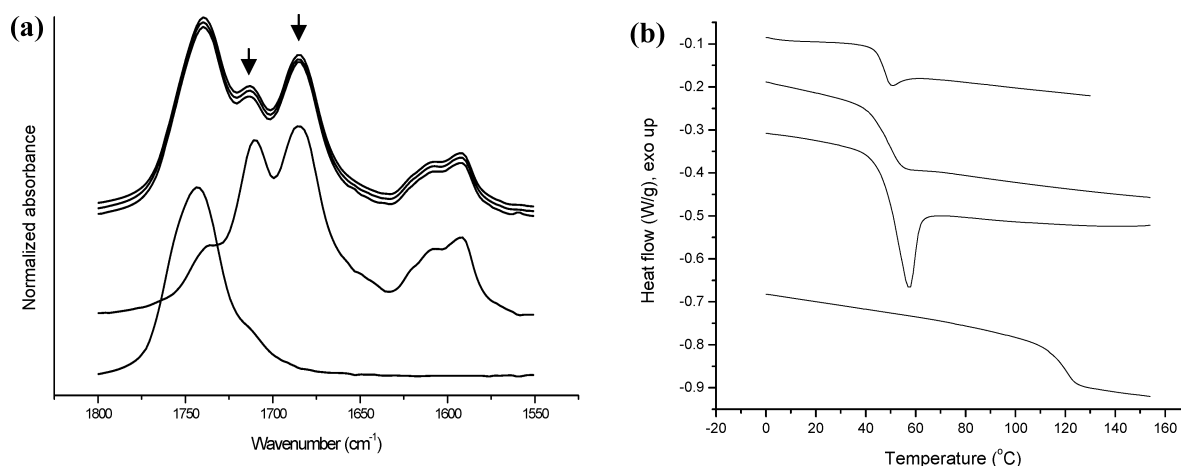


**Figure 9.** (a) IR spectra of the carbonyl region of (from top to bottom) solid dispersion sample containing indomethacin and 50% HPMCAS immediately after preparation, the same sample following storage at 54% RH for 1 day, 84% RH for 1 day, and 94% RH for 1 day, pure amorphous indomethacin, and pure HPMCAS. The relative intensity of the two peaks indicated by arrows were unaffected by exposure to moisture (see text for assignments). (b) DSC thermograms of (from top to bottom) amorphous indomethacin, solid dispersion sample containing indomethacin and 50% HPMCAS, identical solid dispersion sample following 1-day storage at 94% RH and subsequent drying, and pure HPMCAS.

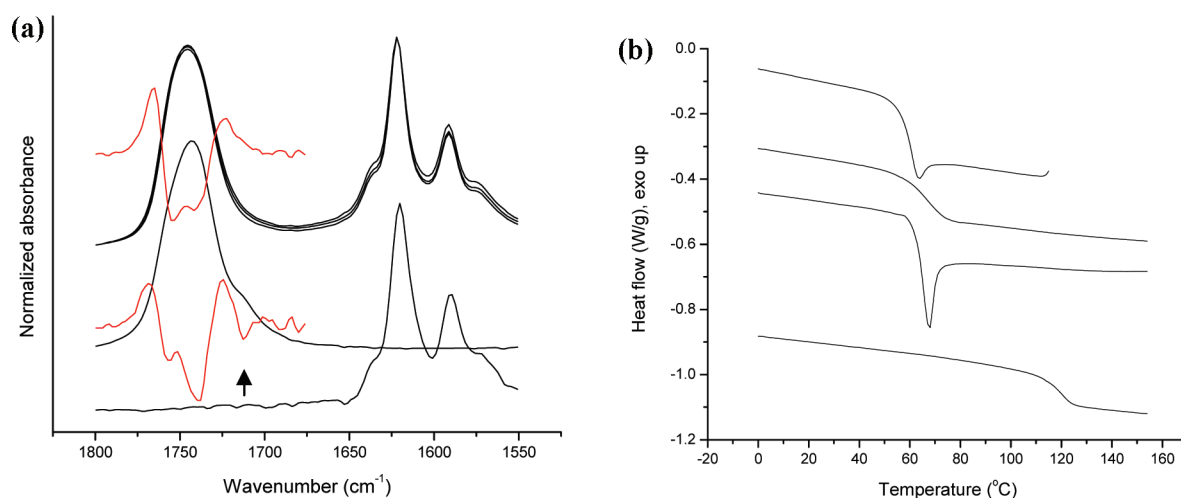


**Figure 10.** (a) IR spectra of the carbonyl region of (from top to bottom) solid dispersion sample containing quinidine and 50% HPMCAS immediately after preparation, after 1-day storage at 75% RH, after 1-day storage at 94% RH, pure amorphous quinidine, and pure HPMCAS. The second derivative profiles (red lines) of the solid dispersion sample (top) after 1-day storage at 94% RH and (bottom) pure HPMCAS are overlaid to highlight the absence of the indicated peak in the solid dispersion spectra, which was unaffected by exposure to moisture. (b) DSC thermograms of (from top to bottom) amorphous quinidine, solid dispersion sample containing quinidine and 50% HPMCAS, identical solid dispersion sample following 1-day storage at 94% RH and subsequent drying, and pure HPMCAS.

in all solid dispersion samples, indicating disruption of polymer–polymer specific interactions by the drug molecules. Storage of the solid dispersion samples at 94% RH did not result in the reappearance of this shoulder (see Figure 10a).

For these four systems, the DSC thermograms following storage at 94% RH and subsequent drying indicated the presence of only one  $T_g$  at approximately the same temperatures as the dry amorphous solid dispersion samples (see Table 3), which was accompanied by an endothermic peak which can be attributed to enthalpic recovery following enthalpy relaxation. Together with the IR results, it can be

concluded that for these systems, exposure to moisture during storage at RHs as high as 94% did not result in disruption of drug–polymer interactions, signifying the presence of a one-phase amorphous solid dispersion systems at all times.

**Moisture Sorbed by Select Amorphous Solid Dispersion Systems at 25 °C/85% RH.** The amount of moisture sorbed by felodipine and quindine amorphous solid dispersion systems following storage at 25 °C and 85% RH are shown in Table 4. For each model drug, it was observed that, at the same drug-to-polymer ratios, the amount of moisture sorbed by PVP-containing samples was higher than the amount of moisture sorbed by PVPVA-containing

**Table 4.** Amount of Moisture Sorbed by Select Amorphous Solid Dispersion Systems Containing 25% Polymer at 25°C/85% RH

amorphous solid dispersion system	moisture sorbed (g of water/100 g of dry solid)
75% felodipine 25% PVP	6.4 <sup>a</sup>
75% felodipine 25% PVPVA	3.6
75% felodipine 25% HPMCAS	2.4 <sup>a</sup>
75% quinidine 25% PVP	5.3
75% quinidine 25% PVPVA	3.4
75% quinidine 25% HPMCAS	2.4

<sup>a</sup> These values were obtained from ref 33, while other values were obtained experimentally.

samples, which in turn sorbed more moisture than the HPMCAS-containing samples.

## Discussion

Many factors are thought to contribute to the inhibition of drug crystallization in amorphous solid dispersions when a polymer is present. These factors include a reduction in the thermodynamic driving force for crystallization,<sup>24</sup> reduction in molecular mobility,<sup>25,26</sup> and molecular coupling due to drug–polymer specific interactions,<sup>27,28</sup> as well as disruption of molecular recognition events required for nucleation and growth of the crystalline phase.<sup>14,29</sup> Regardless of the specific mechanism(s) by which the amorphous drug is stabilized, it is commonly thought that maximum stabilization of the amorphous form of the drug can only be achieved if the drug and the polymer are mixed at the molecular level,<sup>30</sup> forming what is commonly referred to as an amorphous molecular level solid dispersion. This state of molecular level mixing not only should be present immediately after the formation of the solid dispersion but also would ideally be maintained throughout the lifetime of the pharmaceutical product.

However, the presence of the polymer, which is typically hydrophilic in nature, will result in increased amounts of water being absorbed by the amorphous solid dispersion when compared to the amorphous drug alone.<sup>9,31</sup> As mentioned above, the absorption of water into certain amorphous molecular level solid dispersions prepared with PVP has been reported to disrupt molecular level mixing between the drug and the polymer.<sup>9–11</sup> In this study, it has

been demonstrated that dispersions formed with other polymers are also susceptible to moisture-induced phase separation in some instances. In particular, compounds found to be susceptible to moisture-induced demixing with PVP also appear to undergo this phenomenon when molecularly dispersed with the copolymer PVPVA, albeit to a lesser extent. In contrast, systems prepared with HPMCAS appear to be much less vulnerable to this phenomenon and a minor level of phase separation was only observed for one HPMCAS dispersion (pimozide). In a previous study, it was shown that increases in molecular mobility alone (resulting from absorption of moisture and subsequent plasticization) were not sufficient to induce drug–polymer immiscibility in PVP-containing solid dispersions<sup>10</sup> and it was concluded that the thermodynamics of the system have to be considered. The Flory–Huggins model for ternary systems can be used to help qualitatively understand how the thermodynamics of the system change when water is absorbed. Mathematically, the model can be expressed as

$$\frac{\Delta G_{\text{mix}}}{RT} = n_{\text{W}} \ln \phi_{\text{W}} + n_{\text{D}} \ln \phi_{\text{D}} + n_{\text{P}} \ln \phi_{\text{P}} + n_{\text{W}} \phi_{\text{D}} \chi_{\text{WD}} + n_{\text{W}} \phi_{\text{P}} \chi_{\text{WP}} + n_{\text{D}} \phi_{\text{P}} \chi_{\text{DP}} \quad (1)$$

In this equation,  $\Delta G_{\text{mix}}$  is the free energy of mixing for the ternary system,  $R$  is the gas constant,  $T$  is temperature (in kelvins),  $n$  and  $\phi$  are the mole and volume fractions respectively of each component, and  $\chi$  is the binary interaction parameter between the three components in the system: water (W), drug (D), and polymer (P). The first three terms on the right-hand side of the equation represent the combinatorial entropy of mixing ( $\Delta S_{\text{mix}}$ ), while the latter three terms on the right-hand side contain contributions from the enthalpy of mixing ( $\Delta H_{\text{mix}}$ ). To understand why certain model systems in this study are susceptible to moisture-induced immiscibility while others are not, it is helpful to revisit this model.

From eq 1, complete miscibility between the components in a ternary system is expected in systems where  $\Delta G_{\text{mix}}$  is negative, and only one minimum is observed in the profile of  $\Delta G_{\text{mix}}$  when plotted as a function of composition. Assuming the introduction of a new component is favorable to the mixing entropy,<sup>32</sup> then amorphous–amorphous phase separation is only expected in ternary systems with  $\Delta H_{\text{mix}}$  values sufficiently positive to counteract the favorable entropic effects. In the Flory–Huggins model,  $\Delta H_{\text{mix}}$  for the ternary system is determined by the three interaction parameters representing the strength of interactions between the pairs of components in the systems: drug–polymer ( $\chi_{\text{DP}}$ ), drug–water ( $\chi_{\text{WD}}$ ), and water–polymer ( $\chi_{\text{WP}}$ ). Depending on the relative values of the interaction parameters,  $\Delta H_{\text{mix}}$  can be either negative or positive.

The importance of strong drug–polymer interactions in preventing moisture-induced drug–polymer immiscibility

(24) Marsac, P. J.; Shamblin, S. L.; Taylor, L. S. *Pharm. Res.* **2006**, *23*, 2417–2426.

(25) Korhonen, O.; Bhugra, C.; Pikal, M. J. *J. Pharm. Sci.* **2008**, *97*, 3830–3841.

(26) Van den Mooter, G.; Wuyts, M.; Blaton, N.; Busson, R.; Grobet, P.; Augustijns, P.; Kinget, R. *Eur. J. Pharm. Sci.* **2001**, *12*, 261–269.

(27) Aso, Y.; Yoshioka, S. *J. Pharm. Sci.* **2006**, *95*, 318–325.

(28) Bhugra, C.; Pikal, M. J. *J. Pharm. Sci.* **2008**, *97*, 1329–1349.

(29) Yoshioka, M.; Hancock, B. C.; Zografi, G. *J. Pharm. Sci.* **1995**, *84*, 983–986.

(30) Yu, L. *Adv. Drug Delivery Rev.* **2001**, *48*, 27–42.

(31) Crowley, K. J.; Zografi, G. *J. Pharm. Sci.* **2002**, *91*, 2150–2165.

(32) Marcolli, C.; Luo, B. P.; Peter, T. *J. Phys. Chem. A* **2004**, *108*, 2216–2224.

(33) Rumondor, A. C. F. PhD Thesis, Purdue University, West Lafayette, 2009.



was highlighted in a previous study.<sup>10</sup> For all the drug–polymer model systems included in this study, favorable drug–polymer interactions are observed in the form of hydrogen bonding. For PVPVA-containing model systems, evidence for stronger drug–polymer interactions can be found with indomethacin when compared to those formed with felodipine, quinidine, and pimozone. This supposition is supported by analyzing the red shift experienced by the carbonyl peak of the vinylpyrrolidone moiety of PVPVA when hydrogen bonded to the different drugs. In indomethacin–PVPVA, 42–44  $\text{cm}^{-1}$  shifts to lower wavenumbers were observed, greater than the 19–22  $\text{cm}^{-1}$  shifts observed for the other PVPVA-containing solid dispersions investigated. Chemically, indomethacin contains a COOH hydrogen bond donor group. This group is a better hydrogen bond donor compared to the NH group in felodipine and pimozone and the OH group in quinidine, resulting in stronger drug–polymer interactions. Stronger drug–polymer interactions would result in lower values for  $\chi_{\text{DP}}$ , which is reflective of more favorable values of  $\Delta H_{\text{mix}}$  for indomethacin–PVPVA. This analysis supports experimental evidence whereby no evidence for moisture-induced drug–polymer immiscibility was observed for indomethacin–PVPVA, in contrast to the three other model systems; similar results have been reported with PVP-containing model systems.<sup>10</sup>

However, in addition to considering the strength of the drug–polymer interactions, the hygroscopicity of the polymer and the drug–water interactions must also be considered. For example, felodipine–HPMCAS dispersions contain weaker drug–polymer interactions as compared to felodipine–PVP or felodipine–PVPVA systems,<sup>14</sup> however moisture-induced phase separation was not observed. The same trend was also observed for quinidine-containing solid dispersions. Thus consideration of only the drug–polymer interaction cannot explain the absence of moisture-induced drug–polymer demixing in HPMCAS-containing model systems. Instead, it is more appropriate to consider that  $\Delta H_{\text{mix}}$  depends on the three binary interaction parameters: drug–polymer, water–drug and water–polymer (mathematically represented by  $\chi_{\text{DP}}$ ,  $\chi_{\text{WD}}$  and  $\chi_{\text{WP}}$ ). All drugs used in this study are hydrophobic in nature (large positive  $\log P$  as listed in Table 2), such that the  $\chi_{\text{WD}}$  values are expected to be positive (unfavorable to mixing), for example as calculated for indomethacin.<sup>31</sup> However, their relative contributions to  $\Delta H_{\text{mix}}$  depend not only on the values of  $\chi_{\text{WD}}$  but also on the amount of water sorbed ( $n_{\text{W}}$  in eq 1). The amount of water sorbed in turn depends on the hygroscopicity of the solid matrix, which is governed to some extent by the hygroscopicity of the solid dispersion components.<sup>6,9</sup> Among the model polymers used, PVP is the most hygroscopic, while HPMCAS is the least hygroscopic, as can be seen from the moisture sorption profiles for these polymers shown in Figure 11. As a result, at the same drug-to-polymer weight ratio, the amount of water sorbed by PVP-containing solid dispersions is higher than the amount of water sorbed by HPMCAS-containing solid dispersion.<sup>9,33</sup> This would then result in less positive overall contribution to  $\Delta H_{\text{mix}}$ , which may

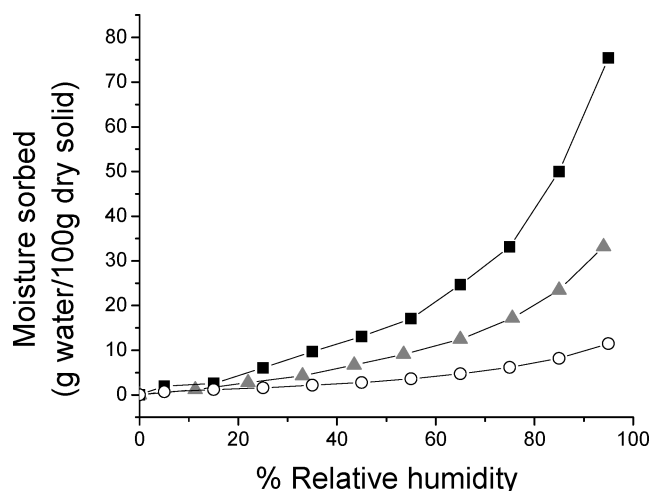


**Figure 11.** Moisture sorption isotherms of (■) PVP, (▲) PVPVA, and (○) HPMCAS at 25 °C, as reported in refs 9, 34.

explain why moisture-induced drug–polymer demixing was observed for felodipine–PVP, felodipine–PVPVA, quinidine–PVP, and quinidine–PVPVA solid dispersions, but not in felodipine–HPMCAS and quinidine–HPMCAS systems. In other words, HPMCAS dispersions simply do not absorb sufficient water to create an unfavorable environment for the hydrophobic drug, and miscibility of the solid dispersion system is maintained. In addition, since HPMCAS-containing amorphous solid dispersions absorb less amounts of moisture compared to their PVP and PVPVA counterparts, it is possible that moisture-induced drug–polymer immiscibility was not observed due to smaller plasticizing effects (or lower molecular mobility). For example, the  $T_g$  of a felodipine–HPMCAS solid dispersion sample containing 25% polymer (by weight) after storage at 75% RH was reported to be around 35 °C, while the  $T_g$  of a comparable felodipine–PVP system was reported around 31 °C.<sup>9</sup>

For felodipine- and quinidine-containing systems, the extent of amorphous–amorphous phase separation following exposure to moisture was more severe for PVP-containing solid dispersions than for the corresponding PVPVA-containing solid dispersions. For example, for felodipine–PVP samples containing 50% (w/w) polymer, storage at 84% RH resulted in a 50% reduction in the intensity of the peak assigned to drug–polymer hydrogen bonding relative to the peak assigned to drug–drug hydrogen bonding. For the comparable PVPVA system, only a 17% reduction in the relative intensity was observed (see Figure 2a). For the quinidine–PVP sample containing 50% polymer, storage at 84% RH resulted in a 47% reduction in the intensity of the peak assigned to drug–polymer hydrogen bonding relative to the free vinylpyrrolidone carbonyl moiety (see Figure 3a). For the comparable PVPVA system, the reduction was only

(34) Taylor, L. S.; Langkilde, F. W.; Zografi, G. J. *Pharm. Sci.* **2001**, 90, 888–901.

(35) Yalkowsky, S. H.; He, Y. *Handbook of Aqueous Solubility Data*; CRC Press: Boca Raton, 2003.

11% (see Figure 4a). For both felodipine- and quinidine-containing model systems, the strength of drug–polymer hydrogen bonding for PVPVA-containing systems is approximately equal to that of their PVP-containing counterparts, as evidenced by similar extents of red shifts observed from the IR spectra. Thus the smaller extent of drug–polymer demixing for PVPVA-containing systems is most likely explained by the reduction in the amount of water sorbed as also shown in Table 4, than by the strength of drug–polymer interactions.

Since pimozone has an NH hydrogen bond donor, a similar strength of drug–polymer interactions is expected as for the felodipine-containing model systems. However, unlike felodipine, evidence for slight moisture-induced drug–polymer demixing was also observed for pimozone–HPMCAS. To explain this behavior, it must be noted that pimozone is the most hydrophobic model drug used in this study, with a log *P* value significantly larger than for the other model drugs chosen (see Table 2). Mathematically, the hydrophobic nature of pimozone would lead to larger  $\chi_{WD}$  values, leading to a larger positive contribution to  $\Delta H_{mix}$ , favoring drug–polymer phase separation even at low amounts of moisture.

## Conclusions

Select amorphous solid dispersion model systems (felodipine–PVPVA, quinidine–PVP, quinidine–PVPVA, pimozone–PVPVA, and pimozone–HPMCAS) were found to undergo amorphous–amorphous phase separation upon exposure to moisture at RHs as low as 54% and as high as

94%. For these systems, water was found to disrupt drug–polymer interactions, which, coupled with the ability of water to increase molecular mobility, led to phase separation. Other model solid dispersion systems (felodipine–HPMCAS, quinidine–HPMCAS, indomethacin–PVPVA, and indomethacin–HPMCAS) remained miscible following equilibration at the highest RH employed, 94% RH. The extent of phase separation was greatest for PVP containing dispersions, less for PVPVA dispersions and, with one exception, not observed for HPMCAS dispersions, and appears to be related to the relative hygroscopicities of the various polymers. It is suggested that the balance between the thermodynamic factors (enthalpy and entropy of mixing) in a ternary water–drug–polymer systems is the important factor in determining which systems are susceptible to moisture-induced drug–polymer demixing. The thermodynamic factors are in turn affected by the amount of water sorbed, which depends on the hygroscopicity of the drug and the polymer as well as the strength of drug–polymer interactions.

**Acknowledgment.** Matthew J. Jackson is gratefully acknowledged for help in collecting IR results. This work was funded by the Dane O. Kildsig Center for Pharmaceutical Processing Research (CPPR), Purdue Research Foundation, and Merck Research Laboratories. This work was supported in part by a grant from the Lilly Endowment, Inc., to Purdue University School of Pharmacy and Pharmaceutical Sciences.

MP9002283